

Self-induced transparency in a flux-qubit chain

Zoran Ivić^{a,b,c,*}, Nikos Lazarides^{b,c}, G.P. Tsironis^{b,c}

^a University of Belgrade, "Vinča" Institute of Nuclear sciences, Laboratory for Theoretical and Condensed Matter Physics, Serbia

^b Crete Center for Quantum Complexity and Nanotechnology, Department of Physics, University of Crete, P. O. Box 2208, Heraklion 71003, Greece

^c National University of Science and Technology MISiS, Leninsky prosp. 4, Moscow 119049, Russia

ARTICLE INFO

Article history:

Received 22 January 2019

Accepted 31 January 2019

Available online 08 February 2019

Keywords:

Self-induced transparency

Superradiance

Soliton

Resonant propagation

ABSTRACT

We introduce a quantum superconducting metamaterial design constituted of flux qubits that operate as artificial atoms and analyze the dynamics of an injected electromagnetic pulse in the system. Qubit-photon interaction affects dramatically the nonlinear photon pulse propagation. We find analytically that the well known atomic phenomenon of self induced transparency may occur in this metamaterial as well and may lead to significant control over the optical pulse propagating properties. Specifically, the pulse may be slowed down substantially or even be stopped. These pulse properties depend crucially on the inhomogeneous broadening of the levels of the artificial atoms.

© 2019 Published by Elsevier Ltd.

This is an open access article under the CC BY-NC-ND license.

(<http://creativecommons.org/licenses/by-nc-nd/4.0/>)

1. Introduction-motivation

The discovery of quantum coherence in mesoscopic and macroscopic systems [1–6] made possible practical applications of quantum mechanical phenomena such as: quantum entanglement, superposition and tunneling in novel quantum technologies including quantum information processing, communication and teleportation [7–16].

A convenient ground for the design of new 'devices' being able to exploit practically quantum mechanical phenomena are engineered materials composed of the artificial "atoms" – quantum bits (qubits). Superconducting qubits, superconducting circuits comprising Josephson junctions (JJ), realize artificial atoms with engineered 'atomic' levels which may be easily tuned by means of external magnetic flux. Owing to that, relatively long coherence times and extremely low dissipation, SCQBs satisfy most of the requirements for being building blocks of viable quantum devices, quantum computers, in particular.

Processing of information stored in qubits demands qubit–qubit mutual communication. It may be realized by direct coupling via the "exchange" interaction of neighboring qubits. Communication between the distant qubits can be achieved exploiting their coupling with electromagnetic radiation. The use of electromagnetic radiation for information processing has two distinct sides. On one

side, the information transfer requires the fast inter-qubit communication. On the other side, the storage as well as manipulation of quantum information requires the significant slowing down of the velocity of the electronic radiation through which qubits communicate. This can be achieved by the coupling of information stored in photon field to excitations in atomic gases [17–27]. In this way coherent information storage in a cold gas (9μK) of sodium atoms [19,28] was accomplished by means of the electromagnetically induced transparency (EIT). In [19] the storage without distortion of the shape of the probe pulse has been demonstrated in excess of 800 μs for weak classical probe pulses, while the nonclassical correlations have been observed for up to 3 μs [28]. This shows a certain promise for the development of photonic quantum information storage devices. However, the storage time scales and retrieval efficiency are still low for these signals.

These difficulties could be overcome through using quantum metamaterials (QMM), i.e artificial optical media composed of a large number of periodically arranged superconducting qubits embedded in superconducting transmission line resonator [29–34]. Exploiting 'meta-atoms' instead of the natural ones, made possible to construct devices operable in regimes which are not accessible with real atoms.

Quantum coherence in ensembles of superconducting qubits may be affected severely by the homogeneous and inhomogeneous broadening of the 'atomic' levels. This is due to coupling with the environment and the fluctuations induced by the non-identity of the JJ units; the latter have non-uniform sizes stemming from fabrication conditions [35–38]. However, relaxation effects do not

* Corresponding author at: National University of Science and Technology MISiS, Leninsky prosp. 4, Moscow 119049, Russia.

E-mail address: zivic@vinca.rs (Z. Ivić).

necessarily lead to a decoherence. Quite on the contrary, the emergence of several quantum coherent phenomena such as photon echo [39–43] and self induced transparency (SIT) [39,44–46], requires *inhomogeneous level broadening*. This implies that inhomogeneous broadening may play positive role in the design of operable quantum devices; for example, spin systems with controllable inhomogeneities were suggested as classical spin echo [47–49] and photon echo memories [42,43,47–50]. Required controllable inhomogeneities may be provided by varying external magnetic field.

In the present work we examine further the possibility of exploiting inhomogeneous broadening in achieving of quantum coherence in engineered superconducting quantum metamaterials. We focus on the emergence of the SIT and soliton like propagation of EM-pulses in QMM. This could be exploited for manipulating EM radiation and development of new techniques of the “light” slowing down with possible application in quantum information processing. For that purpose we propose a “device” – QMM composed of non-interacting flux qubits embedded in massive superconducting resonator. Due to the lack of the offset charge fluctuations, easy control of their energy parameters and the effects of inhomogeneous broadening by means of the external magnetic field, flux qubit based QMMs are more advantageous for practical applications than those based on charge superconducting qubits.

We recall that SIT is lossless propagation of a sufficiently powerful short light pulse through the media consisting of inhomogeneously broadened two-level systems. The crucial theoretical result of the entire concept of SIT, i.e. the area theorem (AT), is strictly valid only for the inhomogeneously broadened media. All features of SIT are determined in terms of single parameter, i.e. the pulse area ($\theta(x) \sim \int_{-\infty}^{\infty} dt' E(x, t')$, $E(x, t')$ – is electric field amplitude.) which measures the strength of the light-matter interaction.¹ Depending on the value of the area SIT exhibits a number of characteristic features: a) pulses with values of area equal to integer multiples of π (i.e. with $\theta_n = n\pi$, $n = 0, 1, 2, \dots$) maintain the same area during the propagation, b) pulses with other values (non-integer ones) must reshape in propagation until their area reaches some θ_n . Pulses with the area corresponding to even (odd) multiples of π are stable (unstable). The changes of the area with the distance of the pulses whose input area is below π is always negative and the media will absorb it. On the contrary, for the pulse whose area is slightly above π , this change is always positive so that $\theta(x)$ increases until it reaches 2π . Pulses having area $2n\pi$ remain unchanged in shape and amplitude and propagates as solitons, while those with area equal to $n = 2, 3, \dots$ split into two, three ... solitons.

Crucial condition for observation of SIT is the coherence between the electric field and two-level systems. It is provided by using so called ultrashort pulses whose duration time is very short with respect to all damping times due to coupling with environment, i.e. due to *homogeneous broadening*. In parallel, pulse duration must be comparable or larger than inhomogeneous broadening relaxation time. Homogeneous broadening is characterized by a relaxation rate which reads: $\frac{1}{T_2} = \frac{1}{2T_1} + \frac{1}{T_2'}$ with T_1 and T_2' being so called longitudinal and transverse relaxation time characterizing, respectively, the decay of “atoms” from excited to ground state and pure dephasing. The inhomogeneous comes from the random distribution of ‘atomic’ transition frequencies. Also, it may arise due to interaction of the qubit degree of freedom with the quasiparticles excitations in the superconductor from which qubit is made of [36]. Quantitative measure of this effect is the dephasing relaxation time T^* . Conditions for the observation of SIT are optimal in

¹ Here we used definition coming from an ‘ordinary’ SIT appearing in atomic gases (vapor), however, as demonstrated below, the pulse area does not strictly refer to the electric field.

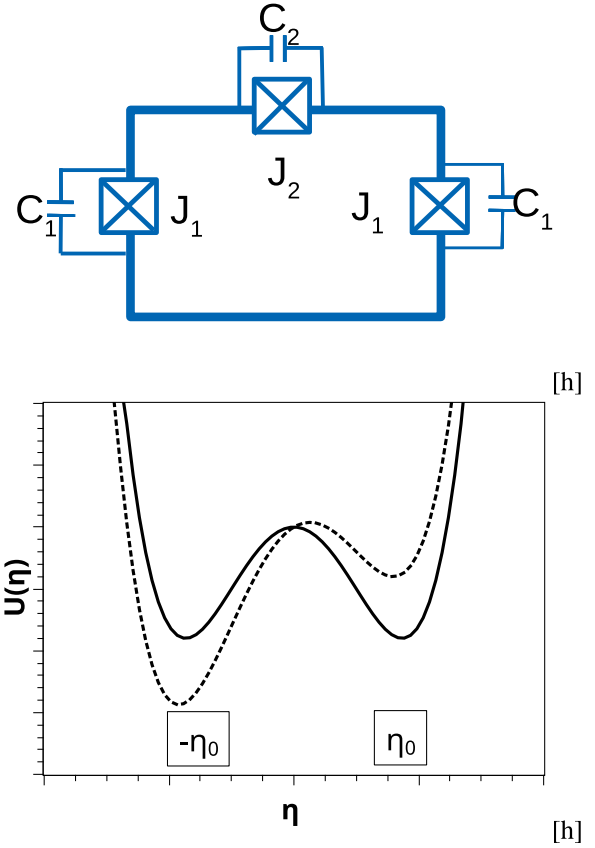


Fig. 1. (a) A three qubit schematic shown with relative phases $\pm\eta$ on superconducting islands, (b) Josephson energy of the system as a function of the relative phase $\eta = \phi_1 - \phi_2$. Phase on JJs are bounded by the condition $\phi_1 - \phi_2 + \phi_3 = 2\pi \frac{\Phi_{ext}}{\Phi_0}$, so that three JJ-junction may be described by relative phase η and $\eta_p = \phi_1 + \phi_2$. Later one is usually chosen as zero [37] and single flux model attains usual double-well form. Solid line: unbiased system with $\Phi = 0.5\Phi_0$; dashed line: system with finite detuning $\delta\phi = \Phi + 0.5\Phi_0$.

the *sharp line limit*

$$\tau_p \ll T_1; T_2' T^* \quad (1)$$

or in *broad line limit*

$$T^* \ll \tau_p \ll T_1; T_2' \quad (2)$$

The structure of this paper is the following: In the next section we describe the proposed design of the metamaterial-based device we study and the associated mathematical model. In Section 3. we discuss the Hamiltonian of the model while in 4-th section we derive and solve in the continuous limit the equations of motion. The role of SIT is uncovered in Section 5. the pulse delay engineering in Section 6. while in Section Appendix B. we conclude.

2. Flux qubit based quantum metamaterial: proposed design and mathematical model

The persistent current qubit [51–54] comprises a superconducting loop interrupted by three Josephson junctions (marked by ‘X’ in Fig. (1. a)). It is taken that the left and right Josephson junctions are identical with capacitance C and charging $E_c = \frac{e^2}{2C}$ and Josephson energy $E_J = \frac{I_c \Phi_0}{2\pi}$, with I_c and Φ_0 being critical current of the side JJs and superconducting flux quantum, respectively. The central junction is characterized by a capacitance αC and Josephson energy αE_J with $\alpha < 1$. The gate capacitances (not shown in the figure) are equal γC .

It was shown in Ref. [51,52] that the phase space coordinate which describes transitions between the right and left states is the relative phase θ of the two superconducting islands Fig. (1). Josephson energies are chosen so that the Josephson part of the Hamiltonian alone defines a bistable system which, at the value of external magnetic flux $\Phi = 0.5\Phi_0$ can be either in the right-hand, or in the left-hand current state. That is, the potential energy of the system as a function of θ has two minima, $\eta = \pm\eta_0$, as shown in Fig. 1(b). These minima are symmetric at $\Phi = 0.5\Phi_0$ and asymmetric at $\Phi \neq 0.5\Phi_0$. By choosing system parameters appropriately, the barrier in the phase space separating the right and left current states can be made low enough, so that tunneling between two classical states will take place. The tunneling amplitude for the barrier $U(\eta)$ is $\Delta \sim \sqrt{\frac{E_J}{E_C}} e^{-\alpha \frac{E_J}{E_C}}$; the detuning of external field from the value $0.5\Phi_0$ produces a bias on the right and left states, making one of them lower in energy than the other: $h = 2I_p(\Phi - 0.5\Phi_0)$ where I_p is the circulating current.

The resulting qubit Hamiltonian is

$$\mathcal{H} = -\Delta\tau_x - h\tau_z. \quad (3)$$

Here $\tau_{x,y,z}$ are Pauli spin matrices in the persistent current basis.

The Hamiltonian (3) may be easily diagonalized in the energy eigenstate basis by means of the unitary transformation:

$$\begin{aligned} \tau_x &= \sigma_x \cos \vartheta + \sigma_z \sin \vartheta, \\ \tau_z &= \sigma_z \cos \vartheta - \sigma_x \sin \vartheta, \\ \tan \vartheta &= \frac{\Delta}{h} \end{aligned} \quad (4)$$

$$H = \epsilon\sigma_z, \quad \epsilon = \sqrt{h^2 + \Delta^2}. \quad (5)$$

Here $-\epsilon$ and ϵ denote the energy of the ground and the first excited states, respectively.

In the notation of Eq. (3) the clockwise ($|+\rangle$) and anticlockwise ($|-\rangle$) current states correspond to qubit ‘spin’ up and down: $\tau_z|\pm\rangle = \pm|\pm\rangle$, while, in the energy eigenbasis ($|e\rangle$ –excited state $|g\rangle$ –ground state) spin up and down corresponds to qubit in excited or in ground state: $\sigma^z|e\rangle = |e\rangle$, and $\sigma^z|g\rangle = -|g\rangle$.

In the operating regime of flux qubit $E_J > E_C$ and near the degeneracy point $\Phi \sim \Phi_0/2$ which provides the preserving of the quantum coherence.

2.1. Qubit – microwave coupling

In order to study the ways of the control over the propagation of electromagnetic radiation we propose that the new device consists of a chain of large number ($N \gg 1$) of aligned equidistant qubits², i.e. forming a the one-dimensional qubit “crystal”. In order to achieve the control over the propagation of photons, it is necessary to couple the QMM with photons. The simplest way to realize it is to embed it in a superconducting cavity [29–34]. A principle scheme of the possible realization of such device with QMM formed of a collection of flux qubits is given below on Fig. 2

In the proposed setup shown in Fig. 2, we associate qubit to a nodes of our quasi one-dimensional “crystal”. To each is assigned a flux variable φ_n , such that the current between the neighboring nodes (n and $n+1$) is given by $((\varphi_{n+1} - \varphi_n)/L)$. We assume that transmission line is homogeneous so that the segments of transmission line between all nodes have identical self-inductance L and capacitance C . The transmission line Hamiltonian has the form [30]:

$$H_{TL} = \frac{1}{2} \sum_n \left[C\dot{\varphi}_n^2 + \frac{1}{L}(\varphi_{n+1} - \varphi_n)^2 \right]. \quad (6)$$

² any type, in principle.

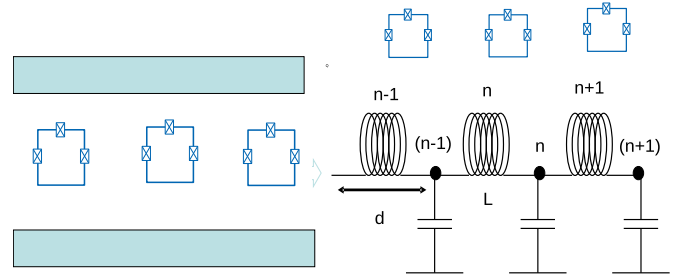


Fig. 2. Possible realizations of the QMM “device”. Large number of flux qubits inductively coupled to superconducting transmission line. Left pane – physical scheme, right pane – representation with lumped-elements circuit. The length of a single section is d , its selfinductance L , and capacitance C . The phase velocity in the unperturbed line is thus $s = d\Omega$, where $\Omega^2 = 1/LC$.

Assuming that each qubit interacts with the part of the resonator, i.e. the nearest neighbouring segments of length a , we may take that $L \equiv L_r$. Electromagnetic radiation travels through the unperturbed line with phase velocity $s = d\Omega$ ($\Omega = 1/\sqrt{LC}$).

The coupling to the qubits takes place due to the fluxes $\varphi_n = M\hat{I}_p(n)$ sent by the n th qubit through the corresponding section of the line, M being their mutual inductance, and $\hat{I}_p \sim \tau_n^z$ the persistent current operator in the qubit loop. That is, the qubit-resonator mode interaction Hamiltonian takes the form:

$$H_i = \sum_n g_n \tau_n^z (\varphi_{n+1} - \varphi_n). \quad (7)$$

with coupling constant $g_n = I_p(n)\sqrt{\Omega/\hbar L}$. The circulating current I_p depends on the amount of external magnetic flux in the loop in units of the flux quantum [52]. In the eigen-energy basis (5) our model Hamiltonian takes the form:

$$H = \sum_n \hbar \frac{\omega_n}{2} \sigma_n^z + \sum_n \frac{g_n}{\epsilon_n} (\Delta_n \sigma_n^x - h_n \sigma_n^z) (\varphi_{n+1} - \varphi_n) + H_{TL}. \quad (8)$$

where the n -indexed parameters (ω_n , Δ_n , h_n) are due to the inhomogeneities introduced by the non-uniform sizes of the JJs which are very sensitive to a fabrication conditions. For that reason, transition frequencies between ground and excited state ($\omega_n = \frac{2\sqrt{\Delta_n^2 + h_n^2}}{\hbar}$) are not the same for all ‘atoms’, but randomly distributed about some mean value. Thus, in practice, any ensemble of superconducting qubits (SCQBs) may be characterized by a normalized line-shape function $\tilde{G}(\omega_n)$. In the large ensembles of qubits this distribution is continuous and lineshape function is determined in such way that $\tilde{G}(\omega_n)d\omega_n$ is the fraction of ‘atoms’ with resonance center frequency within $d\omega_n$ of the frequency ω_n , while the required normalization is $\int_0^\infty \tilde{G}(\omega_n)d\omega_n = 1$ [39].

3. Coupled qubit-photon equations of motion

Propagation of EM radiation in the proposed “device” may be described within the semiclassical approximation: i.e. employing the Hamilton equations for description of the current (voltage) propagation in transmission line, and the Schrödinger equation in order to describe the dynamics of the qubit subsystem. Taking that qubit in each node is in the superposition of ground and excited states we define vector of state of the whole QMM as: $\Psi(t) = \sum_n A_n(t)|e\rangle_n + B_n(t)|g\rangle_n$. Equations of motion for complex functions A_n and B_n may be derived from the Schrödinger equation $i\hbar \frac{\partial}{\partial t} |\Psi(t)\rangle = H|\Psi(t)\rangle$. Since each qubit has only two states, these functions, on each node, satisfy the normalization condition $|A_n|^2 + |B_n|^2 = 1$. Further analysis may be notably simplified introducing the set of new variables, now known as the Bloch vector components, defined as the expectation values of Pauli matrices in the state $\Psi(x, t)$: $S_{x,y,z,n} = \langle \Psi | \sigma_{x,y,z} | \Psi \rangle$ or

explicitly – $S_x = A^*B + c.c.$, $S_y = i(A^*B - c.c.)$, $S_z = |A|^2 - |B|^2$. In terms of Bloch variables normalization condition reads: $\sum_{i=x,y,z} (S_i^n)^2 = 1$.

Bearing in mind that flux qubit operates in the vicinity of the symmetry point ($h_n \ll \Delta_n$) we may neglect the second term in the field-qubit interaction (i.e. the one $\sim \sigma_n^z$) so that the set of evolution (“Maxwell-Bloch”) equations for the proposed model (8) reads:

$$\begin{aligned} \dot{S}_n^x &= -\omega_n S_n^y, \\ \dot{S}_n^y &= \omega_n S_n^x - \frac{g_n}{\hbar} (\varphi_{n+1} - \varphi_n) S_n^z, \\ \dot{S}_n^z &= \frac{g_n}{\hbar} (\varphi_{n+1} - \varphi_n) S_n^y, \\ \ddot{\varphi}_n - \Omega^2 (\varphi_{n+1} + \varphi_{n-1} - 2\varphi_n) &= \frac{g_n}{2C} \langle (S_{n+1}^x - S_n^x) \rangle. \end{aligned} \quad (9)$$

The effects of the *homogeneous* broadening and nonresonant losses in the resonator were ignored by restricting ourselves to the ultrashort pulses with duration far below all relevant relaxation times.

The angular brackets on the right-hand side in the last equation above stands for the accounting for all individual contributions of IH broadened “atoms” each having different transition frequency ω . The ‘atomic’ variables ($S_n^{x,y,z}(t)$) are functions of ω_n , therefore, their collective back-action on propagating pulse is appropriately described in terms of their average values as follows: $\langle S^{x,y,z}(\omega_n) \rangle = \int_0^\infty d\omega_n \tilde{G}(\omega_n) S_n^{x,y,z}(\omega_n)$.

In practical realization of quantum devices, QMM size ($l \sim 1\text{cm}$) highly exceeds that of the individual qubits ($\sim 1\mu\text{m}$) which may be considered as point like objects. Moreover, provided that the wavelength λ of resonator modes is small with respect to scale of transmission line (l), but highly exceeds the inter-qubit separation ($d \ll \lambda < l$), further analytic examination may be performed within the continuum limit. That is, all dynamical variables became continuous functions of time (t) and spatial coordinate along the qubit chain $x: nd \rightarrow x$. Thus (9) becomes

$$\begin{aligned} \dot{S}_x(\varpi) &= -\varpi S_y(\varpi), \quad \dot{S}_y(\varpi) = \varpi S_x(\varpi) - \frac{gL}{\hbar} S_z(\varpi) \mathcal{I}, \\ \dot{S}_z(\varpi) &= \frac{gL}{\hbar} S_y(\varpi) \mathcal{I}, \quad \ddot{x} = s^2 \mathcal{I}'' + \frac{gs^2}{2} \langle S_x'' \rangle, \end{aligned} \quad (10)$$

Here we have introduced a new variable – the current in transmission line corresponding to a spatial variance of the magnetic flux $\mathcal{I}(x, t) = (d/L)\varphi'$ [29,31]. This simple step provides a more transparent physical description of the system dynamics, facilitates calculations and enables us to make bridge with the previous extensive studies of the SIT in atomic gases [44] and SIT of acoustic waves in magnetic materials with paramagnetic impurities [55].³

The new parameter ϖ has the same meaning as ω_n in (13), however, the use of discrete index n in continuum equations could be misleading. Thus, by ϖ here we denote the qubit transition frequency being *different for each qubit*, accordingly, inhomogeneous broadening is described by $\tilde{G}(\varpi)$.

For QMM built of a large number of flux qubits, it is convenient to allow for *continuous* distribution of ϖ -s about mean one (ω_0), which is usually taken to be equal to the carrier pulse frequency $\omega_0 = \omega$. In this case, inhomogeneous broadening is described in terms of so called *detuning* function $\mathcal{G}(D)$ obtained by shifting the ϖ in \tilde{G} towards frequency origin. Thus, $\mathcal{G}(D)dD$ is defined to be the fraction of ‘atoms’, within the detuning

³ For clarity we briefly sketch the derivation of the last equation above. First we write the last equation in 9 in continuum approximation $\ddot{\varphi}(x, t) = s^2 \varphi''(x, t) + \frac{gs}{\hbar} S_x^z(\varpi)$. Now we eliminate φ exploiting $\mathcal{I}_n = (\varphi_{n+1} - \varphi_n)/L \rightarrow \mathcal{I}(x, t) = (d/L)\varphi'$ [29,31], finally taking the spatial derivative of both sides of the wave equation and assuming that the order of the spatial and time derivatives are independent ($\frac{\partial \ddot{\varphi}}{\partial x} = \frac{\partial^2 \dot{\varphi}}{\partial x^2} \equiv \ddot{x}$),

interval dD . Its resonance center frequency ϖ is detuned from the applied field frequency by $D = \varpi - \omega$. Normalization condition now reads: $\int_{-\infty}^\infty \mathcal{G}(D)dD = \int_{-\infty}^\infty \mathcal{G}(D)dD \equiv 1$. Here the first identity holds under the assumption that \mathcal{G} at the true lower limit of integration $D = -\omega$ is so small that the extending this limit towards to $-\infty$ makes no difference.

In practical calculation of the particular averages one should bare in mind that the actual lower limit of integration is $-\omega$, otherwise, averaging the variables being odd functions of D will give result zero.

All dynamical variables in (10) are functions of spatial coordinate and time, but, for the simplicity of presentation, we have used compact notation omitting the arguments (x, t). On the other side, the dependence of the Bloch vector components on ϖ is emphasized as a reminder that due random distribution of the ‘atomic’ frequencies ϖ each qubit is associated with particular ϖ . For that reason, the above system consists of $3N + 1$ evolution equations: three for each of N qubits plus one for the cavity mode. Cavity is described by a single equation since EM pulse “feels” the averaged influence of the all qubits so that flux variables $\varphi(x, t)$ do not depend explicitly on ϖ .

Its solution is extremely difficult task, which, in general may be treated only numerically. Nevertheless, as indicated in numerical simulations [57] and confirmed experimentally [58], SIT in atomic gases and condensed media exhibits essentially the same features in sharp and broad line media. Inhomogeneous broadening influences only the individual velocity of each pulse leaving unaffected all other characteristic properties including soliton like propagation of 2π pulse, its delay, and break up $n2\pi$ pulses into $n2\pi$ pulses. Thus, in practical analytic treatment, one may ignore the inhomogeneous broadening and solve the above system as for the uniform medium consisting of identical atoms. Once when sharp line solutions are known, final solutions for the broadened media, are then obtained by appropriate averaging over the ϖ , or, equivalently, over D .

3.1. Slowly varying envelope and phase approximation

The system of Eq. (10) is formally identical to that appearing in a theoretical treatment of acoustic self-induced transparency (ASIT) [55,56], with \mathcal{I} playing the role of strain. This indicates that, despite the quite different physical content, mathematical treatment of the present problem may be carried on by means of the procedure used in treatment of ASIT [55,56], and SIT in atomic gases employing the slowly varying envelope and phase approximation. It holds provided that dynamical variables in (10) vary slowly over the distances small with respect of the wavelength ($\sim 1/k$) and times of the order of period of resonator modes ($\sim \omega^{-1}$). Under such circumstances we may proceed applying the SVEA and we introduce the set of new dynamical variables

$$\begin{aligned} \mathcal{I}(x, t) &= u(x, t) \cos \Psi(x, t), \quad \Psi = kx - \omega t + \phi(x, t), \\ S_x(x, t) &= P_x(x, t) \cos \Psi(x, t) + P_y(x, t) \sin \Psi(x, t), \\ S_y(x, t) &= P_y(x, t) \cos \Psi(x, t) - P_x(x, t) \sin \Psi(x, t), \end{aligned} \quad (11)$$

where $(u(x, t), \phi(x, t))$ ($P^{x,y,z}$) are slowly varying envelope, phase and components of the new Bloch vector satisfying the following conditions:

$$\begin{aligned} \left| \frac{\partial^2 \mathcal{F}(x, t)}{\partial t^2} \right| &\ll \omega \left| \frac{\partial \mathcal{F}(x, t)}{\partial t} \right| \ll \omega^2 |\mathcal{F}(x, t)| \\ \left| \frac{\partial^2 \mathcal{F}(x, t)}{\partial x^2} \right| &\ll k \left| \frac{\partial \mathcal{F}(x, t)}{\partial x} \right| \ll k^2 |\mathcal{F}(x, t)|. \end{aligned} \quad (12)$$

The symbol $\mathcal{F}(x, t)$ refers either to u , ϕ or on $P_{x,y,z}$.

Now we substitute (11) into (10) and obtain the set of partially reduced MB – equations:

$$\begin{aligned}
\dot{P}_x(D) &= -(D + \dot{\phi})P_y(D), \\
\dot{P}_y(D) &= (D + \dot{\phi})P_x(D) - \frac{gL}{2\hbar}uP_z(D), \\
\dot{P}_z(D) &= \frac{gL}{2\hbar}uP_y(D), \\
\dot{u} + \frac{s^2k}{\omega}u' &= -\frac{gs^2}{4\omega}([k^2P_y(D) + 2k(P'_{x,y}) + \phi'P_y(D)]) \\
u\left(\dot{\phi} + \frac{s^2k}{\omega}\phi' - \frac{\omega^2 - s^2k^2}{2\omega}\right) &= -\frac{gs^2}{4\omega}([k^2P_x - 2k(P'_y - \phi'P_x(D))]).
\end{aligned} \tag{13}$$

In accordance with (12) here we kept only the first-order spatial and time derivatives), while in the final step, the averaging over phase has been performed.⁴ Here $D = \varpi - \omega$ stands for the detuning.

The term “partially reduced” is used here to distinguish system (13) from the known one of the reduced MBEs (RMBE) describing the SIT in atomic gases [39] from which it differs through the explicit dependence of parameters in (13) on carrier wave vector (k) and the appearance terms of the first order of spatial derivatives of Bloch vector components ($P'_{x,y}$) and product of spatial derivative of phase and Bloch vector components ($\phi'P_{x,y}$). They are retained here in order to provide an insight in the degree and nature of approximations involved in derivation of SIT equations and their solutions. In the absence of these terms, system (13) attains simplified form

$$\begin{aligned}
\dot{P}_x &= -(D + \dot{\phi})P_y, \\
\dot{P}_y &= (D + \dot{\phi})P_x - \frac{gL}{2\hbar}uP_z, \\
\dot{P}_z(D) &= \frac{gL}{2\hbar}uP_y(D), \\
\dot{u} + \frac{s^2k}{\omega}u' &= -\left\langle \frac{k^2gL}{4\omega}P_y(D) \right\rangle, \\
u\left(\dot{\phi} + \frac{s^2k}{\omega}\phi' - \frac{\omega^2 - s^2k^2}{2\omega}\right) &= -\left\langle \frac{k^2gL}{4\omega}P_x(D) \right\rangle,
\end{aligned} \tag{14}$$

Apart the explicit appearance of the wave vector of carrier wave (k), the above system of equations is mathematically equivalent to those extensively studied in the context of the theoretical examinations of SIT in atomic gases [39] and condensed media [55]. Owing to that the whole concept now is fairly well elucidated from various points of view although the exact general analytic solutions are yet unknown. We now examine in which degree these achievements hold in the QMMs. Also we explore possible relevance of SIT for the practical applications in novel quantum technologies.

Note that, due to the direct dependence of the effective qubit-field interaction on the carrier pulse wave vector, these known solutions can not be literally copied and used here. In particular, comprehensive study requires solution of the MB-equations together with dispersion law.

We first recall that in resonance ($D = 0$ – the sharp line limit with no inhomogeneous broadening) and in the absence of phase modulation, system (14) may be reduced to sine-Gordon equation providing that all atoms initially in the ground or excited states – $P_z(-\infty) = \pm 1$. Namely, under these conditions first equation of system (14) yields $\dot{P}_x = 0$ implying $P_x = \text{const} \equiv 0$ and the known trigonometric parameterization of Bloch vector components [39,44]: $P_z = P_0 \cos \Theta$ and $P_y = P_0 \sin \Theta$, holds. Note that the normalization condition ($\sum_{i=x,y,z} P_i^2 = 1$) implies $P_0 = P_z(-\infty) \equiv 1$. This “ansatz” yields an important relation connecting the pulse

envelope and Bloch angle:

$$\dot{\Theta} = -\frac{gL}{2\hbar}u. \tag{15}$$

This procedure may be easily generalized to finite detuning and inhomogeneous broadening by means of the McCall–Hahn factorization ansatz. In this way we were able to find comprehensive solutions of MBEs including the explicit form of dispersion law and phase explicitly accounting for inhomogeneous broadening. This method relies on assumption that for finite detunings Bloch vector component P_y only slightly differs from the bare one and reads:

$$P_y = P_0 F(D) \sin \Theta \equiv F(D) P_y(D = 0), \tag{16}$$

where $F(D)$ stands for *spectral – response function* (SRF)⁵. It is yet undetermined and satisfies an obvious normalization condition $F(D = 0) = 1$. In addition, it is required that relation connecting the Bloch angle and pulse envelope (15) still holds. By means of this assumption and ansatz relation (16) which we the third equation of system (13) may be easily integrated resulting in:

$$P_z(\tau) = P_0 \left(1 - F(D) + F(D) \cos \Theta\right). \tag{17}$$

Substitution of (16) in equation for pulse envelope, the fourth one in (14), yields another SG equation

$$\frac{\partial^2 \Theta}{\partial \tau^2} + \frac{s^2k}{\omega} \frac{\partial^2 \Theta}{\partial x \partial \tau} = \frac{k^2 g^2 L^2 \langle F(D) \rangle}{8\omega \hbar P_0} \sin \Theta \tag{18}$$

here $\langle F(D) \rangle \equiv \int_{-\infty}^{\infty} dD G(D) F(D)$. Last equation contains two undetermined quantities k and $F(D)$. They may be evaluated explicitly for the traveling wave tape of solutions. Thus, passing to moving frame $t \rightarrow \tau = t - x/v$, with v being the pulse group velocity, the last equation becomes:

$$\frac{\partial^2 \Theta}{\partial \tau^2} - \tau_p^{-2} \sin \Theta = 0, \quad \tau_p^2 = \frac{8\gamma \hbar \omega P_0}{L^2 g^2 k^2 \langle F(D) \rangle}, \quad \gamma = 1 - \frac{sk^2}{\omega v} \tag{19}$$

Its solution is well known and reads

$$\Theta(\tau) = 4 \arctan e^{-\frac{\tau}{\tau_p}}, \quad u = u_0 \text{sech} \frac{\tau}{\tau_p}, \quad u_0 = \frac{4\hbar}{gL\tau_p}. \tag{20}$$

By direct calculation we found its *area*:

$$\Theta(x) = -\frac{gL}{2\hbar} \int_{-\infty}^{\infty} d\tau u(\tau) \equiv 2\pi, \tag{21}$$

that is, this is a known 2π pulse. Its most intriguing feature is a lossless propagation. To show this explicitly we employ the energy balance equation which we derive from system (14). In the first step we multiply the fourth equation in (14) by u ; then we eliminate uP_y by virtue of the third one, so that we found:

$$\frac{1}{2} \left(\frac{\partial}{\partial t} + \frac{s^2k}{\omega} \frac{\partial}{\partial x} \right) u^2 = -\frac{\hbar k^2}{2\omega} \frac{\partial \langle P_z(D) \rangle}{\partial t}. \tag{22}$$

Finally, integrating it over time we derive the pulse energy loss (gain) per unit length

$$\frac{\partial W}{\partial x} = \alpha (\langle P_0(D) \rangle - \langle P_z(x, D) \rangle), \quad \alpha = \frac{\hbar k}{s^2} \langle F(D) \rangle \tag{23}$$

Here $W = \int_{-\infty}^{\infty} u^2(x, t) dt$ is the density of pulse energy, while $P_0(D) = P_z(-\infty, D) \equiv P_0$ stands for the initial population inversion.

Last relation implies that the incoming pulse may be attenuated or amplified in dependence on the initial preparation of medium. Thus, if initially (before the pulse enters the medium) more “atoms” are in the ground state ($P_0 < 0$ – absorbing medium) than in the excited state, during the propagation, energy is transferred from pulse to medium which becomes excited while pulse is

⁴ This means following formal step $\langle A(\Psi(x, t)) \rangle_\Psi = \frac{1}{2\pi} \int_0^{2\pi} d\psi A(\Psi(x, t))$.

⁵ This is the counterpart of the *Dipole spectral – response function* in the theory of SIT in atomic gases [39].

attenuated. On the other hand, for amplifying media $P_0 > 0$, pulse becomes amplified taking the energy from medium.

This is expected behavior, nevertheless, under the specific conditions pulse exhibits unexpected behavior-loss-less propagation: EM pulse passes through the media with no loss or gain. The easiest way to prove it is to exploit the trigonometric parameterization of Bloch vector components (16) and (17). In such a way we obtain

$$\frac{\partial W}{\partial x} = \alpha P_0 (1 - \cos \Theta). \quad (24)$$

Apparently, pulses with specific values of area – $\Theta = n2\pi$ transit through QMM with no loss or amplification. Nevertheless, lossless propagation is just a particular side of the relationship between the area of the pulse and its features. The most comprehensive insight is provided by the area theorem derived in the *appendix*:

$$\frac{\partial \Theta(x)}{\partial x} = \frac{\beta}{2} \sin \theta, \quad \beta = \frac{g L k}{2\omega} \mathcal{G}(0), \quad (25)$$

its solutions satisfying $\Theta = \Theta_0$ at $x = x_0$ is

$$\tan(\Theta/2) = \tan(\Theta_0/2) e^{\pm(\beta/2)(x-x_0)}. \quad (26)$$

That is, area theorem holds in the present context, so that the pulse propagating in QMM, should exhibit similar features as in the case of SIT in atomic gases [39,44]. In particular, we may expect that, for weak pulses $\Theta_0 \ll \pi$ linear decay of pulse area ($\sim e^{-\beta x}$) would be observed in accordance with the Beer's law. As initial area approaches and exceeds π , fully new features should be observed: for $\Theta \geq \pi$ pulse area does not suffer attenuation during propagation when $\Theta = n\pi$, however pulses whose areas are even (odd) multiples of π are stable (unstable). Here we must note that, at this stage of our analysis, all what was said here is just a hint that these effects may appear in flux based QMM, but, for a definite conclusions knowledge of the wave vector of carrier wave is required. Its evaluation is the subject of next section.

4. Evaluation of dispersion law and phase

Due to the presence of unknown quantities, DSRF, $k(\omega)$ and phase, the above solutions do not give comprehensive picture of EM pulse propagation in QMM. For their evaluation one must go beyond the SG model and must exploit system (14) which we rewrite in terms of new variable $t \rightarrow \tau = t - x/v$:

$$\begin{aligned} P_{x,\tau} &= -(D + \phi_\tau) P_y, \\ P_{y,\tau} &= (D + \phi_\tau) P_x - \frac{Lg}{2\hbar} u P_z, \\ P_{z,\tau} &= \frac{Lg}{2\hbar} u P_y, \\ u_\tau &= -\frac{Lk^2 g}{4\gamma\omega} \langle P_y \rangle, \\ u \left(\phi_\tau - \frac{\omega^2 - s^2 k^2}{2\gamma\omega} \right) &= -\frac{Lk^2 g}{4\gamma\omega} \langle P_x \rangle. \end{aligned} \quad (27)$$

From this system one may determine phase (ϕ) and dispersion law ($k(\omega)$). Note that the phenomenon of SIT, if it can arise at all, is possible in resonance or near it, where $\omega \sim ks$. Otherwise, when $\omega \gg \omega$ or $\omega \ll \omega$ pulse can not excite (de-excite) "atoms" from ground (excited) state and inversion population stays ± 1 "forever", i.e. for time for which pulse passes medium.

Accordingly, we may simplify the above equations in the following way: $s^2 k^2 - \omega^2 = (sk - \omega)(sk + \omega) \approx 2\omega(ks - \omega)$, while $\gamma \rightarrow 1 - s/v$.

We now differentiate the last equation in (27), in which we then substitute $P_{x,\tau}$ from the first equation. This yields

$$\phi_{\tau\tau} + 2\phi_\tau u_\tau - \left(\frac{\omega - sk}{\gamma} - \tilde{D} \right) u_\tau = 0. \quad (28)$$

In approaching this result we transformed average value RHS side of differentiated equation employing the factorization ansatz as follows $\langle DP_y \rangle = \frac{\langle DF(D) \rangle}{F(D)} P_y$. In parallel, in order to eliminate P_y , we use the third equation in (27) which, through the factorization ansatz ($\langle P_y \rangle \equiv \langle F(D) P_y(D=0) \rangle$), is rewritten as

$$P_y = -\frac{4\gamma\omega}{Lgk^2} \frac{F(D)}{\langle F(D) \rangle} u_\tau. \quad (29)$$

Finally, after the integration we have

$$\phi_\tau = \frac{1}{2} \left(\tilde{D} - \frac{\omega - ks}{\gamma} \right), \quad \tilde{D} = \frac{\langle FD \rangle}{\langle F \rangle}. \quad (30)$$

This relation may be used for the determination of the "dispersion relation" $k = k(\omega)$ which is essential for further study, especially for the understanding of the nature and existence of particular types of solutions. At this stage it is possible to put $\phi_\tau = 0$. This is consistent with the *slowly varying phase approximation* according to which ω and k are interpreted as pulse carrier frequency and wave vector. Therefore, ϕ_τ cannot contain a constant part independent of τ .

Otherwise, according to the last equation, phase would renormalize the wave vector and frequency: $k \rightarrow k - \frac{const}{v}$, $\omega \rightarrow \omega + const$. This fully contradicts to the initial demand that $\phi(x, t)$ is slow variable. In this way we easily obtain:

$$k_\pm = \frac{\tilde{D}}{v} \pm \frac{\omega}{s} \sqrt{1 - \frac{2\tilde{D}}{\omega}}, \quad (31)$$

Owing to the preceding discussion near resonance solution reads:

$$k \approx \frac{\omega}{s} - \frac{\tilde{D}}{s} \left(1 - \frac{s}{v} \right). \quad (32)$$

Now, when we have found carrier wave vector and when we established that the phase is constant, we may proceed and evaluate solutions of MBEs. Note that to this end we may use SG equation, however, such solutions contain still undetermined quantity $F(D)$. It may be found from first three equations of system (27) in which we now exploit the fact that $\phi_\tau \equiv 0$.

Substitution of the (17) in the second equation of system (27), where, in accordance with the *factorization ansatz*, we took $P_{y,\tau} = P_0 F(D) \Theta_\tau \cos \Theta$, results in $\Theta_\tau = \frac{D}{1-F(D)} P_x$. Finally, upon differentiating this expression over τ and combining it with the first equation in (27), we found

$$\Theta_{\tau\tau} - \frac{F(D)D^2}{1-F(D)} \sin \Theta = 0. \quad (33)$$

Prefactor in the last expression has dimension of the square of the inverse time, and clearly play the role of reciprocal duration time: $\tau_p^{-2} = \frac{FD^2}{1-F(D)}$. From this expression we found DSRF as

$$F(D) = \frac{1}{1 + (D\tau_p)^2}. \quad (34)$$

For the evaluation of envelope we use system (27) from which we eliminate Bloch vector components and obtain a Φ^3 -type nonlinear evolution equation for envelope. Thus, substituting $\phi_\tau = 0$ in (27) we obtain the following set for next two Bloch vector components.

$$\begin{aligned} P_x &= \frac{DF(D)}{\langle F \rangle} \frac{4\gamma\omega}{Lgk^2} u, \\ P_z &= P_0 - \frac{\gamma\omega}{\hbar k^2} \frac{F(D)}{\langle F(D) \rangle} u^2 \end{aligned} \quad (35)$$

Using the last two equations, and the one for P_x (29) we obtain nonlinear equation for envelope

$$u_{\tau\tau} = \frac{u_0^2}{2}u - u^3, \quad (36)$$

The peak amplitude is given by

$$\begin{aligned} u_0^2 &= \left(\frac{4\hbar}{Lg}\right)^2 \left(\frac{L^2g^2k^2P_0}{8\hbar\omega\gamma} \frac{\langle F(D) \rangle}{F(D)} - D^2\right) \\ &= \frac{2\hbar k^2 P_0}{\omega\gamma} \left\langle \frac{1}{1+D^2\tau_p^2} \right\rangle \equiv \frac{2\hbar k^2 P_0}{\omega\gamma} \langle F(D) \rangle. \end{aligned} \quad (37)$$

Its first integral reads:

$$u_\tau = \frac{ag}{4\hbar} u \sqrt{u_0^2 - u^2}. \quad (38)$$

Its solution is

$$u = u_0 \operatorname{sech} \frac{\tau}{\tau_p}, \quad \tau_p = \frac{4\hbar}{Lg u_0}. \quad (39)$$

Using the above-established relations we found the remaining results:

$$P_x(\tau) = \frac{2D\tau_p P_0}{1 + (\tau_p D)^2} \operatorname{sech} \frac{\tau - \tau_0}{\tau_p}, \quad (a)$$

$$P_y(\tau) = \frac{2P_0}{1 + (\tau_p D)^2} \frac{\tanh \frac{\tau - \tau_0}{\tau_p}}{\cosh \frac{\tau - \tau_0}{\tau_p}}, \quad (b)$$

$$P_z(\tau) = P_0 \left(1 - \frac{2}{1 + (\tau_p D)^2} \operatorname{sech}^2 \frac{\tau - \tau_0}{\tau_p}\right), \quad (c). \quad (40)$$

Finally, the relation connecting pulse velocity and duration time reads.

$$\frac{\gamma}{\left(1 - \frac{\hat{D}}{\omega}\gamma\right)^2} = P_0 \frac{\tau_p^2}{\tau'^2} \langle F(D) \rangle \quad \tau'^2 = \frac{\omega L^2 g^2}{8\hbar s^2} \quad (41)$$

This is quadratic equation for pulse velocity. Existence of its solutions depends on initial conditions: for *attenuator* only subluminal ($v < s$) pulse propagation is possible, while in the *amplifying medium* super-luminal ($v > s$) motion emerges.

In the physically meaningful case, i.e., near the resonance, its approximate solution reads

$$\frac{v}{s} \approx \frac{1 + \frac{2\hat{D}P_0}{\omega} \frac{\tau_p^2}{\tau'^2} \langle F(D) \rangle}{1 - P_0 \left(1 - \frac{2\hat{D}}{\omega}\right) \frac{\tau_p^2}{\tau'^2} \langle F(D) \rangle} \quad (42)$$

5. Pulse delay

Pulse slowing down (absorbing QMM) or acceleration (amplifying QMM) together with lossless propagation is the main feature of the SIT. Now we shall analyze the dependence of pulse velocity on input parameter – pulse duration time.

5.1. Pulse delay in the absence of inhomogeneous broadening

In the sharp-line limit above equation simplifies to

$$\frac{v}{s} \approx \frac{1 + \frac{2\hat{D}P_0}{\omega} \frac{\tau_p^2}{\tau'^2(1+D^2\tau_p^2)}}{1 - P_0 \left(1 - \frac{2\hat{D}}{\omega}\right) \frac{\tau_p^2}{\tau'^2(1+D^2\tau_p^2)}} \quad (43)$$

It is graphically presented in Fig. (3), where we presented the dependence of the pulse velocity on τ_p . The case of ‘attenuator’ ($P_0 = -1$) and ‘amplifier’ are presented in parallel. Note that in the latter case theoretical description of in terms of system (10) is not fully satisfactory. Namely, when ‘atoms’ are excited, processes of spontaneous emission take place. Thus, the decay time, in general,

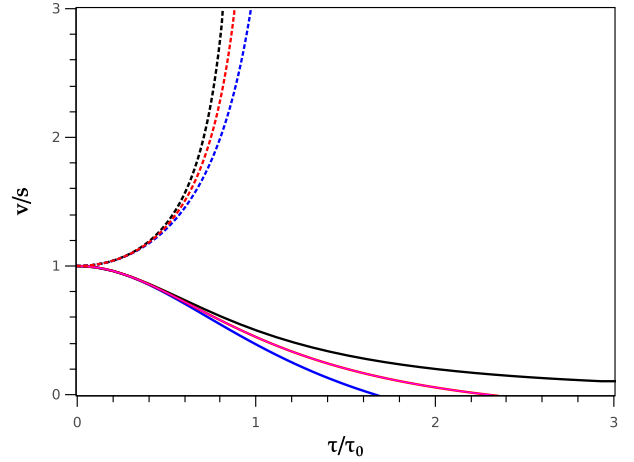


Fig. 3. Illustration of the impact of detuning on the dependence of the pulse velocity on duration time in the sharp line limit. Pulse velocity is measured in units of s , while pulse duration time (τ_p) is measured in units of τ_0 . Full lines correspond to so called pulse in the attenuator, i.e. all qubits in the ground state before pulse enters the system – $P_0 = -1$ at $\tau = -\infty$, while the dotted ones stay for amplifier $P_0 = 1$. Black line corresponds to resonance, while $D\tau_0$ takes 0.1, 0.2 for red, blue curves, respectively. (For interpretation of the references to color in this figure legend, the reader is referred to the web version of this article.)

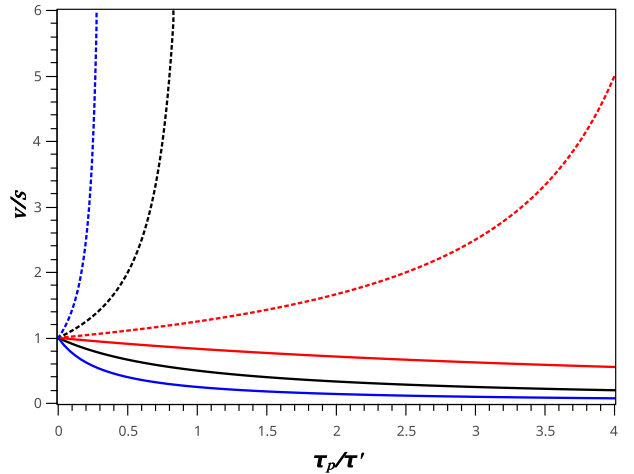


Fig. 4. Pulse velocity vs duration time in the presence of inhomogeneous broadening in the limit $\omega\tau^* > 1$. Black, red and blue lines correspond to τ^*/τ' 1, 0.2 and 3, respectively. (For interpretation of the references to color in this figure legend, the reader is referred to the web version of this article.)

can not be regarded to be small in comparison with pulse duration time. For that reason present results hold only for extremely short pulses, while the realistic description requires accounting for *homogeneous* relaxation explicitly. It may be done by adding relaxation times in system of MBes. For the attenuator, our main result is that detuning may enhance pulse slowing down.

The most interesting result here is that in the proposed device one, in principle, may expect significant slowing down of the EM radiation. It may be even stopped. This is characteristic for flux qubit chain and originates from the ‘dispersion law’ of carrier wave vector, which also, in accordance with (31), imposes condition for the transparency $2\hat{D}/\omega < 1$.

5.2. Impact of inhomogeneous broadening

Size fluctuation of the qubit ensemble with ‘atomic’ transition frequencies centered around mean qubit frequency ω_0 , may be

described by means of the distribution function [45]

$$\mathcal{G}(D) = \frac{1}{\sqrt{2\pi}\sigma} e^{-\frac{D^2}{2\sigma^2}}, \quad \tilde{D} = \varpi - \omega \quad (44)$$

The variance (σ) should be chosen to reproduce experimental data [37,45] – qubit inhomogeneous level broadening full width at half maximum. For a convenience we may introduce the inhomogeneous broadening time $\tau^* \sim 1/\sigma$.

By means of this distribution function we may evaluate required average values $\langle F(D) \rangle$ and \tilde{D} :

$$\begin{aligned} \langle F(D) \rangle &= \frac{\sqrt{2}}{\pi} \frac{\tau^*}{\tau_p} \int_0^\infty \frac{e^{-\frac{z^2}{2\tau_p^2}} dz}{1+z^2}, \\ &\equiv \frac{\tau^*}{\sqrt{2}\tau_p} e^{\left(\frac{T^*}{2\tau_p}\right)^2} \operatorname{erfc}\left(\frac{T^*}{2\tau_p}\right), \quad (z = D\tau_p). \end{aligned} \quad (45)$$

$$\tilde{D} = \frac{1}{4\pi\tau_p} \frac{E_1(Z_0)}{\operatorname{erfc}\left(\frac{T^*}{2\tau_p}\right)}, \quad (46)$$

here $\operatorname{erfc}(x) = \frac{2}{\sqrt{\pi}} \int_x^\infty dt e^{-t^2}$, is the complementary error function, while $E_1(Z_0) = \int_{Z_0}^\infty \frac{e^{-t}}{t} dt$ is exponential integral.

According to our results, pulse properties, its delay (43) in particular, depend substantially on the ratio of the characteristic inhomogeneous broadening relaxation time $T^* \sim 1/\sigma$ and pulse duration. In the broad “line” limit $\tau^* \gg \tau_p$, above average values approaches

$$\langle F(D) \rangle \approx \frac{\tau^*}{\sqrt{2}\tau_p}, \quad \tilde{D} \approx \frac{E_1\left(\frac{\omega^2\tau^{*2}}{2}\right)}{2\pi\tau_p}, \quad (47)$$

and the pulse velocity in units of s approaches:

$$\frac{v}{s} \approx \frac{1 + P_0 \frac{E_1\left(\frac{\omega^2\tau^{*2}}{2}\right)\tau^*}{\sqrt{2\pi}\omega\tau'^2}}{1 - \frac{P_0}{\sqrt{2}} \left(1 - \frac{E_1\left(\frac{\omega^2\tau^{*2}}{2}\right)}{\sqrt{2\pi}\omega\tau_p}\right) \frac{\tau_p\tau^*}{\tau'^2}} \quad (48)$$

The above result imply that the pulse delay substantially depends on the ratio of carrier wave period of oscillation ($\sim 1/\omega$) and the scale of the pulse broadening τ^* . In particular, for small values of $\omega\tau^*$, exponential integral diverges, while rapidly tends to zero in the opposite limit. In the latter case normalized velocity (v/s) versus duration time attains simple form:

$$\frac{v}{s} \approx \frac{1}{1 - P_0 \frac{\tau^* \tau_p}{\tau'}}, \quad (49)$$

which is practically identical to a corresponding relation in the context of SIT in media composed of natural atoms, atomic vapors, for example [39,44]. In the present context ratio τ^*/τ' defines the degree of the impact of inhomogeneous broadening on pulse delay. Thus sharper distribution is more influential than the broad one.

In the opposite limit, $\omega\tau^* \rightarrow 0$, exponential integral highly diverges. Nevertheless, for each particular finite, no matter how small, value of $\omega\tau^*$, E_1 may attain large enough values, so that the numerator in (48) can go to zero. That is, pulse may be stopped. To illustrate it we picked $\omega\tau^*/2 \sim 0.0707$ for which $E_1 \sim \sqrt{2\pi}$. Now velocity–duration time relation reads:

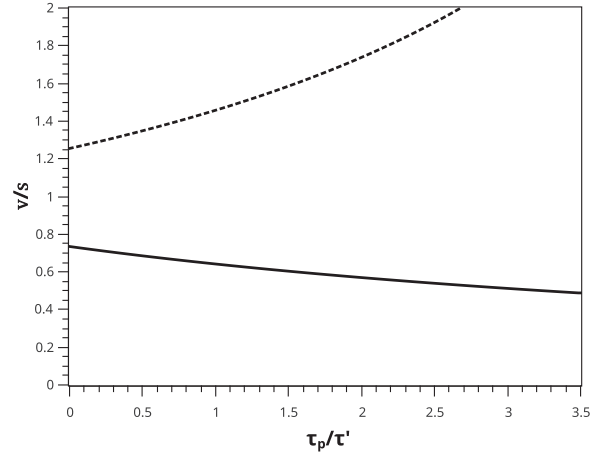


Fig. 5. Illustration of the dependence of the velocity on duration time in the limit: $\omega\tau^* \rightarrow 0$. Full line corresponds to absorbing media, while a dotted one represents amplifying ones.

$$\frac{v}{s} \approx \frac{1 + 7P_0 \frac{\tau^{*2}}{\tau'^2}}{1 - \frac{P_0}{\sqrt{2}} \frac{\tau_p}{\tau'} \frac{\tau^*}{\tau'} + \frac{P_0}{2} \frac{\tau^{*2}}{\tau'^2}}. \quad (50)$$

In Fig. (5) we have plotted velocity duration time dependence in the limit $\omega\tau^* \rightarrow 0$. The main difference with respect to previous case is the appearance of the maximal (minimal for amplifying medium) velocity. It is determined by the values of physical parameters, essentially depends on the broadening time τ^* . For the special case we considered here it tends towards $v \approx 1 + 7P_0 \frac{\tau^{*2}}{\tau'^2}$.

5.3. Behaviour of the Beer's law coefficients

One of the most interesting features of the SIT pulse propagating in QMM is the dependence of the absorption coefficient on the pulse duration time. This is the consequence of the dispersion law (32). Thus, exploiting that relation, absorption coefficient in (25) becomes:

$$\beta = \beta_0 \left(1 - P_0 \langle F(D) \rangle \frac{\tilde{D}}{\omega} \frac{\tau_p^2}{\tau'^2}\right), \quad \beta_0 = \frac{\operatorname{Lg}\mathcal{G}(0)}{2s}. \quad (51)$$

In the sharp line limit we predict some very interesting results. In the absorbing media ($P_0 = -1$) absorption coefficient increases with the rise of the pulse duration. Wider pulses are more absorbed than the sharp ones. In the amplifying media ($P_0 = 1$) opposite behaviour is observed. This coefficient, which now corresponds to pulse amplification, decreases with pulse width: sharper pulses are more amplified than the wide ones. This is illustrated on (6) where the dependence of absorption (amplification) coefficient on soliton duration time is sketched. One of the most intriguing result is vanishing of the amplification coefficient: for each pulse for which condition $D/\omega > D^2\tau'^2$ is satisfied, there appear a critical value of the duration time, for which β approaches zero.

Such behaviour is quite different than in the case of an ordinary SIT where pulse duration has no any impact on its amplification or absorption.

In the case finite broadening absorption (amplification) coefficient very weakly depends on pulse duration as can be seen from the explicit expression

$$\beta \approx \beta \left(1 - \frac{P_0}{2\sqrt{2\pi}} \frac{\tau^*}{\omega\tau'^2} e^{\left(\frac{\tau^*}{\sqrt{2}\tau_p}\right)^2} E_1(z_0)\right), \quad (52)$$

where, due to the restriction imposed by the condition ($\tau_p \gg \tau^*$) absorption coefficient practically does not depend on pulse width. Nevertheless, it is still pretty different from the corresponding

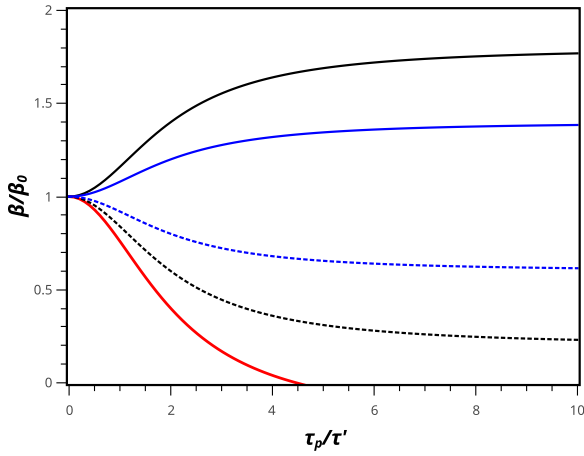


Fig. 6. Illustration of the “Beer’s coefficient” on pulse width. Dotted (full) lines correspond to amplifier (absorber) in all cases we took $D/\omega = 1/2$ while $D^2\tau'^2$ takes values, 0.5, 1 and 1.2 for blue, red and black, lines, respectively, respectively. (For interpretation of the references to color in this figure legend, the reader is referred to the web version of this article.)

quantities in ordinary SIT, but the width of the inhomogeneous broadening distribution takes role of pulse duration. In particular, since the exponential integral does not depend on τ^* , coefficient β is linear function of τ^* , decreasing for absorbing media and increasing for amplifying. As $\omega\tau'$ rises, E_1 rapidly approaches zero and $\beta \rightarrow \beta_0$.

6. Concluding remarks

We have demonstrated that relaxation phenomena, specifically inhomogeneous broadening of the energy levels of the artificial atoms (qubits), may be used in order to achieve and maintain quantum coherence in complex systems built of a large number of superconducting qubits. For that purpose we have exploited the fact that the emergence of some quantum coherent phenomena, self induced transparency, in particular, require inhomogeneous broadening of ‘atomic’ levels. We propose that the self-induced transparency may be observed in a quantum metamaterial built of the large number of flux-qubits inductively coupled to superconducting transmission line. In-homogeneity of the flux qubit energy levels arises due to fluctuations of the sizes of JJ units stemming from the fabrication conditions. In contrast to ordinary SIT in atomic gasses where it corresponds to dissipation-less transmission of light pulse, here we predicted analogous effect but for the propagation of electric current through the transmission line.

One of the most intriguing consequence of the self-induced transparency in flux – qubit based QMMs is the possibility to control the pulse velocity on demand. The main benefit is the significant slowing down of the pulse. For some values of system parameters it may be even stopped.

Necessary control may be provided by varying flux-qubit resonant frequency by means the external field. Thus, one may use the external magnetic field in order to control the degree of inhomogeneous broadening. According to [61] it is necessary to fabricate control lines to apply magnetic flux on the qubits and this will enable one to tune the resonant frequency of each qubit. We hope that the pulse velocity management that is predicted in the present work would provide an interesting experimental problem for practical quantum superconducting metamaterials.

Acknowledgments

This work was partially supported by the [Ministry of Education, Science and Technological Development of Republic Serbia](#), Grants No. III – 45010 and OI – 171009, the Ministry of Science and Higher Education of the Russian Federation in the framework of Increase Competitiveness Program of NUST “MISIS” (No. K2-2017-006), implemented by a governmental decree dated 16th of March 2013, N 211. NL also acknowledges support by [General Secretariat for Research and Technology](#) (GSRT) and the Hellenic Foundation for Research and Innovation (HFRI) (Grant no.: 203).

Appendix A. Derivation of the area theorem

We exploit the system (14) where we integrate the fourth equation over time from $-\infty$ to ∞ . This yields

$$\frac{\partial \theta}{\partial x} = \left\langle \frac{L^2 g^2 k}{8 \hbar} \int_{-\infty}^{\infty} dt P_y(x, t; D) \right\rangle = \quad (53)$$

$$\frac{L^2 g^2}{8 \hbar s^2} \int_{-\infty}^{\infty} dD \mathcal{G}(D) \int_{-\infty}^{\infty} k P_y(x, t; D) \quad (54)$$

For the mathematical convenience we now introduce an auxiliary variable $S_D(x, t) = P_x + iP_y$ which, by virtue of the first two equations of system (14), satisfies the following evolution equation:

$$\frac{\partial S_D}{\partial t} = \dot{\Omega} S_D - i \frac{Lg}{2\hbar} u P_z, \quad \Omega(t) = (D + i\Gamma)t + \phi(t) \quad (55)$$

The presences of phase time derivative ($\dot{\phi}(t)$) in (59) and complex detuning $\Omega - i\Gamma$ indicate, respectively, the accounting for of the pulse chirping and the homogeneous broadening – due to transverse relaxation $\Gamma = 1/T_2$. It is here introduced *ad hock* (by hand) and corresponds to simplified description of relaxation processes by adding phenomenological damping terms in Eq. (14).

We now proceed in a manner of Lamb [59,60] formally integrating the above equation

$$S_D = S_h(t) - i \frac{Lg}{2\hbar} \int_{-\infty}^t u(x, t') P_z(x, t') e^{i(\Omega(t) - \Omega(t'))} dt' \quad (56)$$

S_h stands for the homogeneous solution. This is critical point since, according to huge literature on AT, there are two quite different ways how to proceed. That is, according to original approach of McCall and Hahn [44], only homogeneous part matters and should be included in handling the integration in (56), while in latter work only the particular part was taken into account.

In handling the integration we now assume that the aforementioned conditions for the observation of the SIT specified through (1) or (2) are satisfied. In either case there exist a widely separated time scales characterizing a different physical processes and facilitate the evaluation the time integral. It may be seen more clearly after the transition to new variable $\tau = t - t'$ so that the last expression becomes:

$$S_D = S_h(t) - i \frac{Lg}{2\hbar} \int_0^\infty u(x, t - \tau) P_z(x, t - \tau) e^{i(\Omega(t) - \Omega(t - \tau))} d\tau.$$

Under the aforementioned conditions amplitude, phase, and population inversion are slow variables, as compared with exponential part which rapidly oscillates. Thus, for all of them we may take $\mathcal{F}(x, t - \tau) \approx \mathcal{F}(x, t)$ and we have approximate result:

$$S_D \approx iu(x, t) P_z(x, t) \int_0^\infty e^{-i(D - i\Gamma)\tau} d\tau.$$

After that the integral of the exponential factor is trivial, giving the well known singular form:

$$\frac{1}{iD + \Gamma} \rightarrow \mathcal{P} \frac{-i}{D} + \pi \delta(D) \quad (57)$$

Separating real and imaginary part we obtain

$$P_x(x, t) \approx u(x, t)P_z(x, t)\mathcal{P}\frac{1}{D} \\ \implies \lim_{\Gamma \rightarrow 0} \frac{D}{D^2 + \Gamma^2} u(x, t)P_z(x, t) \quad (58)$$

$$P_y(x, t) = \pi \delta(D)u(x, t)P_z(x, t) \quad (59)$$

$$\frac{\partial \theta}{\partial x} = \frac{L^2 k g^2}{8 \hbar s^2} \mathcal{G}(0) \int_{-\infty}^{\infty} u(x, t; D=0)P_z(x, t; D=0)dt. \quad (60)$$

In the resonance, which is obviously the case, $u(x, t) = \frac{2\hbar}{Lg} \dot{\Theta}$, while $P_z = P_0 \cos \Theta$, that is $u(x, t; D=0)P_z(x, t; D=0) = \frac{2\hbar}{Lg} P_0 \dot{\Theta} \cos \Theta \equiv \frac{2\hbar}{Lg} P_0 \frac{\partial}{\partial t} \sin \Theta$ and the integral in the above equation is easily evaluated and the known form of area theorem is approached:

$$\frac{\partial \theta}{\partial x} = \frac{\beta}{2} \sin \theta, \quad \beta = \frac{Lgk}{2s^2} \mathcal{G}(0) \quad (61)$$

In addition, by virtue of the above explicit expression for P_x fifth equation defining the phase modulation becomes

$$\left(\dot{\phi} + \frac{s^2 k}{\omega} \phi' - \frac{\omega^2 - s^2 k^2}{2\omega} \right) = - \left(\frac{Lg}{8 \hbar s^2} \frac{\Gamma}{kD^2 + \Gamma^2} P_z(x, t; D) \right), \quad (62)$$

Appendix B. Derivation of average values

We focus on evaluation of $\tilde{D} = \frac{\langle F(D)D \rangle}{\langle F(D) \rangle}$.

By direct substitution corresponding expressions in the above formula we have:

$$\tilde{D} = \frac{1}{\sqrt{2\pi} \langle F(D) \rangle} \int_{-\omega}^{\infty} \frac{De^{-\frac{D^2}{2\sigma^2}}}{1 + (\tau_p D)^2} dD \quad (63)$$

In order to avoid the meaningless – zeroth result of integration, here we had to use the true lower limit of integration ($-\omega$) instead of the extended one ($-\infty$). In order to evaluate explicitly this integral we had to perform three subsequent substitution of integration variable. First we introduce $y = \tau_p D$, after which the lower integration limit became $-\omega \tau_p$, while, the resulting integral is of the same form as the original one with redefined coefficients. In the second step following replacement is introduced: $z = 1 + y^2$. This yields:

$$\tilde{D} = \frac{1}{\sqrt{2\pi} \langle F(D) \rangle} \frac{\tau^*}{2\tau_p^2} \int_{1+(\omega\tau_p)^2}^{\infty} \frac{e^{-\left(\frac{\tau^*}{\sqrt{2}\tau_p}\right)^2}}{z} dz \quad (64)$$

Finally, after the substitution $Z = \left(\frac{\tau^*}{\sqrt{2}\tau_p}\right)^2 z$, last expression may be written through the *exponential integral* as follows:

$$\tilde{D} = \frac{1}{\sqrt{2\pi} \langle F(D) \rangle} \frac{\tau^*}{2\tau_p^2} e^{\left(\frac{\tau^*}{\sqrt{2}\tau_p}\right)^2} E_1(Z_0), \\ Z_0 = \left[1 + (\omega\tau_p)^2 \right] \left(\frac{\tau^*}{\sqrt{2}\tau_p} \right)^2 \quad (65)$$

where

$$E_1(Z_0) = \int_{Z_0}^{\infty} dZ \frac{e^{-Z}}{Z} \quad (66)$$

References

- [1] Martinis JM, Devoret MH, Clarke J. Energy-level quantization in the zero-voltage state of a current-biased Josephson junction. *Phys Rev Lett* 1985;55:1543–6.
- [2] Yu Y, Han SY, Chu X, S-I C, Wang Z. Coherent temporal oscillations of macroscopic quantum states in a Josephson junction. *Science* 2002;296:889–92.
- [3] Leggett AJ. Macroscopic quantum coherence and decoherence in SQUIDS. In: Averin DV, Ruggiero B, Silvestrini P, editors. *Macroscopic quantum coherence and quantum computing*. New York: Springer Science+Business Media; 2001. p. 1.
- [4] Friedman JR, Patel V, Chen W, Tolpygo SK, Lukens JE. Quantum superposition of distinct macroscopic states. *Nature* 2000;406:43–6.
- [5] Nakamura Y, Pashkin Y u A, Tsai JS. Quantum-state interference in a cooper-pair box. In: Averin DV, Ruggiero B, Silvestrini P, editors. *Macroscopic quantum coherence and quantum computing*. New York: Springer Science+Business Media; 2001. p. 17.
- [6] van der WCH, ter Haar ACJ, Wilhelm FK, Schouten RN, Harmans CJPM, Orlando TP, Lloyd S, Mooij JE. Quantum superposition of macroscopic persistent-current states. *Science* 2000;290:773–7.
- [7] DiVincenzo DP. Quantum computation. *Science* 1995;270:255–61.
- [8] DiVincenzo DP. *Fortschr Phys* 2000;48: 771–78
- [9] Kaminsky WM, Lloyd S. Scalable architecture for adiabatic quantum computing of NP-hard problems. In: Leggett AJ, Ruggiero B, Silvestrini P, editors. *Quantum computing and quantum bits in mesoscopic systems*. New York: Kluwer Academic; 2004. p. 229–36.
- [10] Imamoğlu A, Awschalom DD, Burkard G, DiVincenzo DP, Loss D, Sherwin M, Small A. Quantum information processing using quantum dot spins and cavity-QED. *Phys Rev Lett* 1999;83:4204–7.
- [11] Devoret MH, Schoelkopf RJ. Superconducting circuits for quantum information: an outlook. *Science* 2013;339:1169–74.
- [12] Georgescu IM, Ashhab S, Nori F. Quantum simulation. *Rev Mod Phys* 2014;86:153.
- [13] Paraoanu GS. Recent progress in quantum simulation using superconducting circuits. *J Low Temp Phys* 2014;175:633.
- [14] Cao Y, Li Y-H, Cao Z, Yin J, Chen Y-A, Yin H-L, Chen T-Y, Ma X, Peng C-Z, Jian-Wei P. Direct counterfactual communication via quantum zeno effect. *PNAS* 2017;114:4920–4.
- [15] Bennett CH. Teleporting an unknown quantum state via dual classical and Einstein-Podolsky-Rosen channels. *Phys Rev Lett* 1993;70:1895–9.
- [16] Pirandola S, Eisert J, Weedbrook C, Furusawa A, Braunstein SL. Advances in quantum teleportation. *Nat Photon* 2015;9:641–52.
- [17] Ginsberg NS, Garner SR, Hau LV. Coherent control of optical information with matter wave dynamics. *Nature* 2007;445:623–6.
- [18] Hau LV, Harris SE, Dutton Z, Behroozi CH. Light speed reduction to 17 metres per second in an ultracold atomic gas. *Nature* 1999;397:594–8.
- [19] Liu C, Dutton Z, Behroozi CH, Hau LV. Observation of coherent optical information storage in an atomic medium using halted light pulses. *Nature* 2001;409:490.
- [20] Bajcsy M, Zibrov AS, Lukin MD. Stationary pulses of light in an atomic medium. *Nature* 2003;426:638.
- [21] L-M D, Lukin MD, Cirac JI, Zoller P. Long-distance quantum communication with atomic ensembles and linear optics. *Nature* 2001;414:413–18.
- [22] Lukin MD, Imamoğlu A. Controlling photons using electromagnetically induced transparency. *Nature* 2001;413:273–6.
- [23] Phillips DF, Fleischhauer A, Mair A, Walsworth RL, Lukin MD. Storage of light in atomic vapor. *Phys Rev Lett* 2001;86:783–6.
- [24] Liu C, Dutton Z, Behroozi CH, Hau LV. Observation of coherent optical information storage in an atomic medium using halted light pulses. *Nature* 2001;409:490–3.
- [25] Heinze G, Hubrich C, Halfmann T. Stopped light and image storage by electromagnetically induced transparency up to the regime of one minute. *Phys Rev Lett* 2013;111(033601):5.
- [26] Fleischhauer M, Lukin MD. Dark-state polaritons in electromagnetically induced transparency. *Phys Rev Lett* 2000;84:5094–7.
- [27] Zimmer FE, André A, Lukin MD, Fleischhauer M. Coherent control of stationary light pulses. *Opt Commun* 2006;264:441–53.
- [28] van der WCH, Eisaman MD, André A, Walsworth RL, Phillips DF, Zibrov AS, Lukin MD. Atomic memory for correlated photon states. *Science* 2003;301:196–200.
- [29] Zagoskin AM, Rakhmanov AL, Savel'ev S, Nori F. Quantum metamaterials: electromagnetic waves in josephson qubit lines. *Phys Status Solidi B* 2009;246:955–60.
- [30] Rakhmanov AL, Zagoskin AM, Savel'ev S, Nori F. Quantum metamaterials: electromagnetic waves in a josephson qubit line. *Phys Rev B* 2008;77(144507):7.
- [31] Zagoskin AM. *Quantum engineering: theory and design of quantum coherent structures*. Cambridge University Press; 2011.
- [32] Macha P, Oelsner G, J-M R, Marthaler M, André S, Schön G, Hübner U, H-G M, Il'ichev E, Ustinov AV. Implementation of a quantum metamaterial using superconducting qubits. *Nat Commun* 2014;5(5146):6.
- [33] Shulga KV, Il'ichev E, Fistul MV, Besedin IS, Butz S, Astafiev OV, Hübner U, Ustinov AV. Magnetically induced transparency of a quantum metamaterial composed of twin flux qubits. *Nat Commun* 2018;9(150):6.
- [34] Ivić Z, Lazarides N, Tsironis GP. Qubit lattice coherence induced by electromagnetic pulses in superconducting metamaterials. *Sci Rep* 2016;6(29374):8.

- [35] Wendin G, Shumeiko VS. Quantum bits with Josephson junction (review article). *Low Temp Phys* 2007;33:724.
- [36] Catelani G, Nigg SE, Girvin SM, Schoelkopf RJ, Glazman. Decoherence of superconducting qubits caused by quasiparticle tunneling. *Phys Rev B* 2012;86:184514.
- [37] Lambert N, Matsuzaki Y, Kakuyanagi K, Ishida N, Saito S, Nori F. Superradiance with an ensemble of superconducting flux qubits. *Phys Rev B* 2016;94:224510.
- [38] Koppenhöfer M, Marthaler M, Schön G. Superconducting quantum metamaterials as an active lasing medium: effects of disorder. *Phys Rev B* 2016;93:063808.
- [39] Allen L, Eberly JH. *Optical resonance and two-level atoms*. New York: Wiley; 1975.
- [40] Kopvillem UKh, Nagibarov VR. Light echo on paramagnetic crystals. *Fiz Metall Metalloved* 1963;15:313.
- [41] Kurnit NA, Abella ID, Hartmann SR. Observation of a photon echo. *Phys Rev Lett* 1964;13:567–70.
- [42] Moiseev SA. Photon-echo-based quantum memory of arbitrary light field states. *J Phys B* 2007;40:3877–91.
- [43] Tittel W. Photon-echo quantum memory in solid state systems. *Laser Photon Rev* 2010;4:244.
- [44] McCall SL, Hahn EL. Self-induced transparency by pulsed coherent light. *Phys Rev Lett* 1967;18:908–11.
- [45] Panzarini G, Hohenester U, Molinari E. Self-induced transparency in semiconductor quantum dots. *Phys Rev B* 2002;65:165322.
- [46] Adamashvili G.T., Weber C., Knorr A., Adamashvili N.T. *Phys Rev A* 75:063808.
- [47] Wasenberg JH, Ardavan A, Briggs GAD, Morton JLL, Schoelkopf RJ, Schuster DI, Mølmer K. Quantum computing with an electron spin ensemble. *Phys Rev Lett* 2009;103:070502.
- [48] Wasenberg JH, Kurucz Z, Mølmer K. Dynamics of the collective modes of an inhomogeneous spin ensemble in a cavity. *Phys Rev A* 2011;83:023826.
- [49] Zhukov AA, Shapiro DS, Pogosov WV, Lozovik YuE. Dynamics of a mesoscopic qubit ensemble coupled to a cavity: role of collective dark states. *Phys Rev A* 2017;96:033804.
- [50] Nakajima T, Delbecq MR, Otsuka T, Amaha S, Yoneda J, Noiri A, Takeda K, Allison G, Ludwig A, Wieck AD, Hu X, Nori F, Tarucha S. Coherent transfer of electron spin correlations assisted by dephasing noise. *Nat Commun* 2018;9:2133.
- [51] Mooij JE, Orlando TP, Levitov L, Tian L, van der WCH, Lloyd S. Josephson persistent current qubit. *Science* 1999;285: 1036–9.
- [52] You JQ, Hu X, Ashhab S, Nori F. Low-decoherence flux qubit. *Phys Rev B* 2007;75:140515.
- [53] Yan F, Gustavsson S, Kamal A, Birenbaum J, Sears AP, Hover D, Gudmundsen TJ, Rosenberg D, Samach G, Weber S, Yoder JL, Orlando TP, Clarke J, Kerman AJ, Oliver WD. The flux qubit revisited to enhance coherence and reproducibility. *Nat Commun* 2016;7:12964.
- [54] Levitov LS, Orlando TP, Majer JB, Mooij JE. Quantum spin chains and Majorana states in arrays of coupled qubits. *ArXiv:cond-mat/0108266* [cond-mat.mes-hall].
- [55] Denisenko GA. The propagation of a short acoustic pulse in a medium containing paramagnetic centers. *Zh Eksp Teor Fiz* 1971;60:2269–73.
- [56] Adamashvili GT. The theory of acoustic self-induced transparency in magneto-ordered mediums. *Solid State Commun* 1981;40:623–7.
- [57] Estes LE, Etesonand DC, Narducci LM. *IEEE J Quantum Electron* 1970;QE-6:546.
- [58] Gibbs HM, Slusher RE. Sharp line self-induced transparency. *Phys Rev A* 1972;6:2326.
- [59] Lamb Jr GL. Analytical descriptions of ultrashort optical pulse propagation in a resonant medium. *Rev Mod Phys* 1971;43:99–124.
- [60] Lamb Jr GL. *Elements of soliton theory*. *Rev Mod Phys* 1971;43:99–124. Wiley Interscience Publication, John Wiley & Sons, New York, Chichester, Brisbane, Toronto, 1980.
- [61] Matsuzaki Y, Kakuyanagi K, Toida H, Yamaguchi H, Munro WJ, Saito S. Coherent coupling between 4300 superconducting flux qubits and a microwave resonator. *NTT Tech Rev Feature Articl* 2017;15(7).